BUCKLING ANALYSIS OF GRID-STIFFENED COMPOSITE CYLINDRICAL SHELL

R. Velmurugan* and M. Buragohain**

Abstract

An energy based smeared stiffener model is developed to obtain equivalent stiffness coefficients of a general grid-stiffened composite cylindrical shell. These equivalent stiffness coefficients are used in the Ritz buckling analysis of the shell. Transverse shear properties are important in a stiffened shell and results are obtained for First order Shear Deformation Theory (FSDT) as well as for Classical Laminated Shell Theory (CLST). Parametric study is carried out to find out the effects of various design parameters on specific buckling load of the shell.

***Key words** : Grid-stiffened Composite Shell, Buckling Analysis*

Notations

a = spacing of helical ribs

$\mathbf{A}$, $\mathbf{B}$, $\mathbf{D}$, $\mathbf{S}$ = extensional stiffness matrix, extension-bending coupling stiffness matrix, bending stiffness matrix and transverse shear stiffness matrix respectively for the ribs / skins

$\mathbf{A^*}$, $\mathbf{B^*}$, $\mathbf{D^*}$, $\mathbf{S^*}$ = extensional compliance matrix, extension-bending coupling compliance matrix, bending compliance matrix and transverse shear compliance matrix respectively for the ribs / skins

$\mathbf{A_{eq}}$, $\mathbf{B_{eq}}$, $\mathbf{D_{eq}}$, $\mathbf{S_{eq}}$ = extensional stiffness matrix, extension-bending coupling stiffness matrix, bending stiffness matrix and transverse shear stiffness matrix respectively for the equivalent shell

$\mathbf{A^*_{eq}}$, $\mathbf{B^*_{eq}}$ $\mathbf{D^*_{eq}}$, $\mathbf{S^*_{eq}}$ = extensional compliance matrix, extension-bending coupling compliance matrix, bending compliance matrix and transverse shear compliance matrix respectively for the equivalent shell

A_{ij}, B_{ij} D_{ij}, S_{ij} = elements of stiffness matrices of the stiffening ribs / skin

A_{ijeq}, B_{ijeq} D_{ijeq}, S_{ijeq} = elements of stiffness matrices of the equivalent shell

b_a, b_c, b_h = cross-sectional widths of axial, circumferential and helical ribs respectively

D = diameter of the shell

h_k = z co-ordinate of the k^{th} ply

k = shear correction factor

L = length of the shell

m, n = half wave numbers

M_x, M_y, M_{xy} = moments per unit length applied on the system of stiffening members

M_{xeq}, M_{yeq}, M_{xyeq} = moments per unit length of the equivalent shell

n_a, n_c, n_h = numbers of axial, circumferential and helical ribs respectively

$\mathbf{N, M, Q}$ = vectors of unit in-plane forces, moments and transverse forces respectively for the ribs / skins

$\mathbf{N_{eq}}$, $\mathbf{M_{eq}}$ $\mathbf{Q_{eq}}$ = vectors of unit in-plane forces, moments and transverse forces respectively for the equivalent shell

N_x, N_y, N_{xy} = in-plane forces per unit length applied on the system of stiffening members

N_{xeq}, N_{yeq}, N_{xyeq} = in-plane forces per unit length of the equivalent shell

Q_{xz}, Q_{yz} = transverse forces per unit length applied on the system of stiffening members

Q_{xzeq} Q_{yzeq} = transverse forces per unit length of the equivalent shell

* Department of Aerospace Engineering and Composites Technology Centre, Indian Institute of Technology Madras Chennai-600 036, India

** Advanced Systems Laboratory (ASL), Kanchanbagh Post, Hyderabad-500 058, India

Manuscript received on 13 Oct 2006; Paper reviewed, revised and accepted on 18 Jun 2007

$\overline{\mathbf{Q}}$ = reduced transformed stiffness matrix of the composite laminate making the ribs / skins

R_s, R = radii of the imaginary cylinder through the system of stiffening members and the equivalent shell

u, v, w = displacements at a point (x,y,z) in the x, y, z directions respectively

u_o, v_o, w_o = displacements at a point in the mid-plane

U, V, Π = strain energy, work done by external forces and total potential energy respectively of the shell

U_{mn}, V_{mn} W_{mn}, R_{mn}, T_{mn} = amplitudes of generalized displacements

x, y, z = axial, circumferential and radial co-ordinates as per cylindrical co-ordinate system (Fig.1)

ϕ_x , ϕ_y = rotations of transverse normal

ε_x , ε_y , γ_{xy} = in-plane normal and shear strains

γ_{yz} , γ_{xz} = transverse shear strains

ε_x^0 , ε_y^0 , γ_{xy}^0 = in-plane normal and shear strains in the mid-plane

γ_{yz}^0 , γ_{xz}^0 = transverse shear strains in the mid-plane

ε_x^1 , ε_y^1 , γ_{xy}^1 = changes in curvatures in mid-plane

ε^0, ε^1, γ = vectors of in-plane strains, changes in curvatures and transverse strains respectively

Δ = surface area

θ = angle of orientation of helical ribs w. r. t. meridian

Introduction

Cylindrical shells are used in many aerospace and other high end applications that demand weight efficiency. A common loading condition for such a structure is axial compression. In these applications, buckling behavior of the structure is of critical importance. Composite shells, in general, and composite grid-stiffened shells, in particular, provide very high specific strength and stiffness properties making them very attractive in such applications. In these shells a grid of stiffening ribs is made by filament winding along grooves cut in foam or plaster layer on a metallic mandrel. Either an inner skin or an outer skin or both are laid by filament winding. In certain applications no skin is used. The stiffening ribs are basically unidirectional composite and they form a very efficient system of load bearing elements. As a result, grid-stiffened composite shells provide better buckling resistance and there is a growing interest in them; but they still are a subject of relatively recent origin.

Vasiliev et. al [1] give a note on the development of grid-stiffened composite shells. A design and analysis procedure that considers transverse shear properties is discussed. Initial design/analysis is based on a continuum model where stiffening ribs are smeared to arrive at an equivalent shell. Three basic methods are used in the buckling analysis of a stiffened shell (i) smeared stiffener model, (ii) discrete model and (iii) branched plate and shell model. Smeared stiffener approach is based on mathematical models that smear the stiffening ribs into an equivalent ply. This is very efficient in global buckling analysis and especially useful to narrow down the choice of design elements in the initial design phase. Several authors [1-7] have adopted the smearing approach in buckling analysis of stiffened shells. Vasiliev et. al [1] and Jones [2] have used rib spacing in relation to rib cross sectional width as the criterion to smear the ribs. Wodesenbet et. al [3] and Kidane et. al [4] present a global buckling analysis model wherein smeared stiffener approach is used through force/moment analysis of a unit cell to determine stiffness contribution of the stiffeners. Transverse strain and shear strains are neglected. An improved smeared stiffener model that accounts for transverse shear flexibility is used by Jaunky et. al [5, 6] and Damodar et. al [7]. In this model skin-stiffener interaction effects are included by considering a neutral surface profile of the skin-stiffener combination. Smearing criterion is based on equivalence of strain energies and the method involves considering the strain energies of the skin and stiffeners through the use of strain compatibility equations. Slinchenko et. al [8] used the smearing approach, on the basis of rib spacing, to determine structural stiffness matrix for finite element analysis of grid-stiffened structure. The discrete approach and branched plate/shell approach are computationally more involved and these methods are normally used in the final design phase of a grid-stiffened shell. Several authors have worked in these directions e.g. Huybrechts et. al [9] and Wang [10].

Issues involved in buckling analysis of composite structures are complex and the subject is still evolving as is evident from a large number of publications that are appearing regularly. For example Jaunky et. al [11] give

an assessment of shell theories as applied to buckling of cylindrical laminated composite shell. Geier et al [12] present some simple solutions for buckling behavior of cylindrical shell.

Publications on grid-stiffened shell are limited and a sizable portion of it is on FEA, manufacturing and testing. Finite element analysis of grid-stiffened shells is complex and time consuming and it is difficult to accommodate changes in the grid configuration [8]. Filament wound composite grid-stiffened shells throw up numerous possible design configurations in terms various design elements e.g. (i) types of stiffening ribs - helical, circumferential, axial or a combination thereof, (ii) number of ribs, (iii) cross sectional details, (iv) spacing of ribs, (v) skin details, etc. In the initial design phase, wherein broad choice of design elements is made, one needs to consider numerous possible configurations. FEA in such a situation is time consuming and it is more economical to use a quick tool such as smeared stiffener model to find global buckling load.

The primary aim of this work is to present a simple and efficient analytical model for global buckling analysis that would be useful in the initial design phase. A cylindrical composite shell stiffened by a grid of continuous ribs is considered. Smearing the ribs into an equivalent shell is done by equating the strain energy of the stiffened shell to that of the equivalent shell and the methodology involves use of stress/moment resultants in the formulation of strain energy. Ritz buckling analysis of the equivalent composite shell is carried out to find out the critical buckling load as well as the mode shapes. Due to the presence of several parameters optimal design of a grid-stiffened shell is always a challenge. In this work, all the design parameters mentioned in the previous paragraph have been considered; thus, effect of change in any of the design parameters on the final buckling response can be readily found out. Towards this a parametric study is carried out as an aid and broad conclusions are arrived at. Transverse shear properties are important in a stiffened shell and transverse shear terms are included in the formulations. Results as per CLST and those as per FSDT are compared.

Analytical Formulation

Kinematic Relations

Classical Laminated Plate/Shell Theory is based on the following displacement field [13]:

$$\begin{Bmatrix} u(x,y,z) \\ v(x,y,z) \\ w(x,y,z) \end{Bmatrix} = \begin{Bmatrix} u_0(x,y) - z\dfrac{\partial w_0}{\partial x} \\ v_0(x,y) - z\dfrac{\partial w_0}{\partial y} \\ w_0(x,y) \end{Bmatrix} \quad (1)$$

Displacements and the co-ordinate directions are defined in Fig.1. Following Kirchhoff hypothesis,

$\varepsilon_z = \gamma_{xz} = \gamma_{yz} = 0$ and the strain-displacement relations for CLST are given by :

$$\begin{Bmatrix} \varepsilon_x^0 \\ \varepsilon_y^0 \\ \gamma_{xy}^0 \\ \varepsilon_x^1 \\ \varepsilon_y^1 \\ \gamma_{xy}^1 \end{Bmatrix} = \begin{Bmatrix} \dfrac{\partial u_0}{\partial x} \\ \dfrac{\partial v_0}{\partial y} + \dfrac{w_0}{R} \\ \dfrac{\partial v_0}{\partial x} + \dfrac{\partial u_0}{\partial y} \\ -\dfrac{\partial^2 w_0}{\partial x^2} \\ -\dfrac{\partial^2 w_0}{\partial y^2} \\ -2\dfrac{\partial^2 w_0}{\partial x\,\partial y} \end{Bmatrix} \quad (2)$$

The strains are given by :

$$\begin{Bmatrix} \varepsilon_x \\ \varepsilon_y \\ \gamma_{xy} \end{Bmatrix} = \begin{Bmatrix} \varepsilon_x^0 \\ \varepsilon_y^0 \\ \gamma_{xy}^0 \end{Bmatrix} + z \begin{Bmatrix} \varepsilon_x^1 \\ \varepsilon_y^1 \\ \gamma_{xy}^1 \end{Bmatrix} \quad (3)$$

In the First order Shear Deformation Theory, the assumption regarding perpendicularity of a tranverse normal to the laminate mid-plane is relaxed and the displacement field for a cylindrical shell is obtained as :

$$\begin{Bmatrix} u(x,y,z) \\ v(x,y,z) \\ w(x,y,z) \end{Bmatrix} = \begin{Bmatrix} u_0(x,y) + z\phi_x(x,y) \\ v_0(x,y) + z\phi_y(x,y) \\ w_0(x,y) \end{Bmatrix} \quad (4)$$

Consequently, the strain-displacement relations for FSDT are given by :

$$\begin{Bmatrix} \varepsilon_x^0 \\ \varepsilon_y^0 \\ \gamma_{xy}^0 \\ \gamma_{yz}^0 \\ \gamma_{xz}^0 \\ \varepsilon_x^1 \\ \varepsilon_y^1 \\ \gamma_{xy}^1 \end{Bmatrix} = \begin{Bmatrix} \dfrac{\partial u_0}{\partial x} \\ \dfrac{\partial v_0}{\partial y} + \dfrac{w_0}{R} \\ \dfrac{\partial v_0}{\partial x} + \dfrac{\partial u_0}{\partial y} \\ \dfrac{\partial w_0}{\partial y} + \phi_y - C_1 \dfrac{v_0}{R} \\ \dfrac{\partial w_0}{\partial x} + \phi_y \\ -\dfrac{\partial^2 w_0}{\partial x^2} \\ -\dfrac{\partial^2 w_0}{\partial y^2} \\ \dfrac{\partial \phi_x}{\partial y} + \dfrac{\partial \phi_y}{\partial y} + \dfrac{C_2}{2R}\left(\dfrac{\partial v_0}{\partial x} - \dfrac{\partial u_0}{\partial y}\right) \end{Bmatrix} \quad (5)$$

where C_1 and C_2 are 'tracer' coefficients that take the values as follows [11] :

$C_1 = 1, C_2 = 1$ Sanders-Koiter shell theory

$C_1 = 1, C_2 = 0$ Love's shell theory

$C_1 = 0, C_2 = 0$ Donnell's shell theory

The strains are given by :

$$\begin{Bmatrix} \varepsilon_x \\ \varepsilon_y \\ \gamma_{xy} \\ \gamma_{yz} \\ \gamma_{xz} \end{Bmatrix} = \begin{Bmatrix} \varepsilon_x^0 \\ \varepsilon_y^0 \\ \gamma_{xy}^0 \\ \gamma_{yz}^0 \\ \gamma_{xz}^0 \end{Bmatrix} + z \begin{Bmatrix} \varepsilon_x^1 \\ \varepsilon_y^1 \\ \gamma_{xy}^1 \\ 0 \\ 0 \end{Bmatrix} \quad (6)$$

Constitutive Relations

In the Classical Laminate Plate/Shell theory, the transverse shear terms do not appear and the linear constitutive relations can be expressed as :

$$\begin{Bmatrix} \mathbf{N} \\ \mathbf{M} \end{Bmatrix} = \begin{bmatrix} \mathbf{A} & \mathbf{B} \\ \mathbf{B} & \mathbf{D} \end{bmatrix} \begin{Bmatrix} \varepsilon^0 \\ \varepsilon^1 \end{Bmatrix} \quad (7)$$

Transverse shear terms are included in the First order Shear Deformation Theory and the constitutive relations are modified as :

$$\begin{Bmatrix} \mathbf{N} \\ \mathbf{M} \\ \mathbf{Q} \end{Bmatrix} = \begin{bmatrix} \mathbf{A} & \boldsymbol{B} & \mathbf{0} \\ \mathbf{B} & \boldsymbol{D} & \mathbf{0} \\ \mathbf{0} & \mathbf{0} & \mathbf{S} \end{bmatrix} \begin{Bmatrix} \varepsilon^0 \\ \varepsilon^1 \\ \gamma \end{Bmatrix} \quad (8)$$

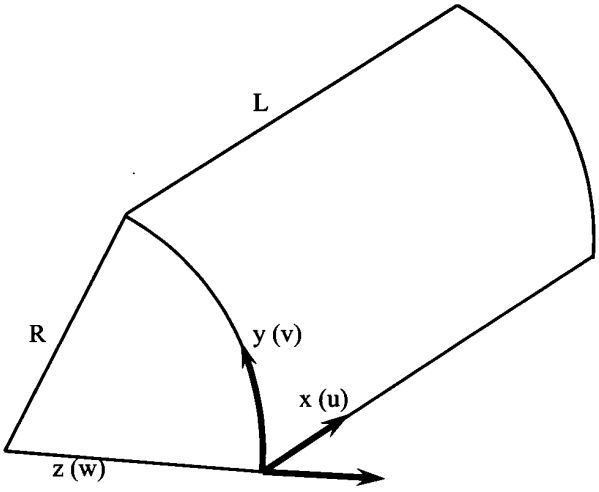

Fig.1 Co-ordinate system and displacements

The vectors and matrices in Eqn. (7) and Eqn. (8) are defined as :

$$\mathbf{N} = \begin{Bmatrix} N_x \\ N_y \\ N_{xy} \end{Bmatrix}, \ \mathbf{M} = \begin{Bmatrix} M_x \\ M_y \\ M_{xy} \end{Bmatrix}, \ \mathbf{Q} + \begin{Bmatrix} Q_{yz} \\ Q_{xz} \end{Bmatrix}$$

$$A_{ij} = \sum_{k=1}^{n} \overline{Q}_{ij}^{k} \ (h_k - h_{k+1}) \qquad i, j = 1, 2, 3$$

$$B_{ij} = \frac{1}{2} \sum_{k=1}^{n} \overline{Q}_{ij}^{k} \ (h_k^2 - h_{k+1}^2) \qquad i, j = 1, 2, 3$$

$$D_{ij} = \frac{1}{3} \sum_{k=1}^{n} \overline{Q}_{ij}^{k} \ (h_k^3 - h_{k+1}^3) \qquad i, j = 1, 2, 3$$

$$S_{ij} = \sum_{k=1}^{n} \overline{Q}_{ij}^{k} \ (h_k - h_{k+1}) \qquad i, j = 4, 5$$

$$\{\varepsilon^0\} = \begin{Bmatrix} \varepsilon_x^0 \\ \varepsilon_y^0 \\ \gamma_{xy}^0 \end{Bmatrix}, \ \{\varepsilon^1\} = \begin{Bmatrix} \varepsilon_x^1 \\ \varepsilon_y^1 \\ \gamma_{xy}^1 \end{Bmatrix}, \ \{\gamma\} = \begin{Bmatrix} \gamma_{yx}^0 \\ \gamma_{xz}^0 \end{Bmatrix} \tag{9}$$

Energy Formulations

The total potential energy of the grid stiffened composite shell is given by the sum of the strain energy and work done by external forces.

$$\Pi = U + V \tag{10}$$

Strain energy is given by :

$$U = \frac{1}{2} \int\int\int \left(\sigma_x \varepsilon_x + \sigma_y \varepsilon_y + \sigma_z \varepsilon_z + \tau_{xy} \gamma_{xy} + \tau_{yz} \gamma_{yz} + \tau_{xz} \gamma_{xz} \right) dz \, dx \, dy \tag{11}$$

In Classical Laminate Plate/Shell Theory, transverse shear strains are zero and we obtain the following :

$$U = \frac{1}{2} \int\int \left(N_x \varepsilon_x^0 + N_y \varepsilon_y^0 + N_{xy} \gamma_{xy}^0 + M_x \varepsilon_x^1 + M_y \varepsilon_y^1 + M_{xy} \varepsilon_{xy}^1 \right) dx \, dy \tag{12}$$

Then, using Eqn. (7) we get the following :

$$\begin{aligned} U = {} & \frac{\Delta}{2} \left[(A_{11}^* N_x^2 + A_{22}^* N_y^2 + A_{66}^* N_{xy}^2) \right] \\ & + 2 \ (A_{12}^* N_x N_y + A_{16}^* N_x N_{xy} + A_{26}^* N_y N_{xy}) \\ & + 2 \ (B_{11}^* N_x M_x + B_{22}^* N_y M_y + B_{66}^* N_{xy} M_{xy}) \\ & + 2 \ (B_{12}^* N_x M_y + B_{21}^* N_y M_x + B_{16}^* N_x M_{xy}) \\ & + 2 \ (B_{61}^* N_{xy} M_x + B_{26}^* N_y M_{xy} + B_{62}^* N_{xy} M_y) \\ & + (D_{11}^* M_x^2 + D_{22}^* M_y^2 + D_{66}^* M_{xy}^2) \\ & + 2 \left[(D_{12}^* M_x M_y + D_{16}^* M_y M_{xy} + D_{26}^* M_y M_{xy}) \right] \end{aligned} \tag{13}$$

In the First order Shear Deformation theory, transverse shear strains are included and we get the following :

$$\begin{aligned} U = {} & \frac{1}{2} \int\int \left(N_x \varepsilon_x^0 + N_y \varepsilon_y^0 + N_{xy} \gamma_{xy}^0 \right. \\ & + M_x \varepsilon_x^1 + M_y \varepsilon_y^1 + M_{xy} \varepsilon_{xy}^1 \\ & \left. + N_{yz} \gamma_{yz}^0 / k + N_{xz} \gamma_{xz}^0 / k \right) dx \, dy \end{aligned} \tag{14}$$

and

$$\begin{aligned} U = {} & \frac{\Delta}{2} \left[(A_{11}^* N_x^2 + A_{22}^* N_y^2 + A_{66}^* N_{xy}^2) \right] \\ & + 2 \ (A_{12}^* N_x N_y + A_{16}^* N_x N_{xy} + A_{26}^* N_y N_{xy}) \\ & + 2 \ (B_{11}^* N_x M_x + B_{22}^* N_y M_y + B_{66}^* N_{xy} M_{xy}) \\ & + 2 \ (B_{12}^* N_x M_y + B_{21}^* N_y M_x + B_{16}^* N_x M_{xy}) \\ & + 2 \ (B_{61}^* N_{xy} M_x + B_{26}^* N_y M_{xy} + B_{62}^* N_{xy} M_y) \\ & + (D_{11}^* M_x^2 + D_{22}^* M_y^2 + D_{66}^* M_{xy}^2) \\ & + 2 \ (D_{12}^* M_x M_y + D_{16}^* M_y M_{xy} + D_{26}^* M_y M_{xy}) \\ & + \left[(A_{44}^* N_{yz}^2 + A_{556}^* N_{xz}^2 + 2 A_{45}^* N_{xz} N M_{yz}) / k^2 \right] \end{aligned} \tag{15}$$

A convenient way to express the strain energy for Ritz buckling analysis is in terms of the generalized strain vector and stiffness matrix:

For CLST :

$$U = \int_0^{2\pi R}\int_0^{L} \begin{Bmatrix} \varepsilon^0 \\ \varepsilon^1 \end{Bmatrix} \begin{bmatrix} \mathbf{A} & \mathbf{B} \\ \mathbf{B} & \mathbf{D} \end{bmatrix} \begin{Bmatrix} \varepsilon^0 \\ \varepsilon^1 \end{Bmatrix} dx\, dy \qquad (16)$$

and, for FSDT :

$$U = \int_0^{2\pi R}\int_0^{L} \begin{Bmatrix} \varepsilon^0 \\ \varepsilon^1 \\ \gamma \end{Bmatrix} \begin{bmatrix} \mathbf{A} & \boldsymbol{B} & \mathbf{0} \\ \mathbf{B} & \boldsymbol{D} & \mathbf{0} \\ \mathbf{0} & \mathbf{0} & \mathbf{S} \end{bmatrix} \begin{Bmatrix} \varepsilon^0 \\ \varepsilon^1 \\ \gamma \end{Bmatrix} dx\, dy \qquad (17)$$

The work done by in-plane loads are given by [14] :

$$V = \int_0^{2\pi R}\int_0^{L} \left[N_x \left(\frac{\partial w}{\partial x}\right)^2 + N_y \left(\frac{\partial w}{\partial y}\right)^2 \right] + \left[N_{xy} \left(\frac{\partial w}{\partial x}\ \frac{\partial w}{\partial y}\right) \right] dx\, dy \qquad (18)$$

Smeared Stiffener Model

Figure 2 shows a sector of a cylindrical system of helical, axial and circumferential stiffening members. This system is converted into a set of equivalent plies (Fig.3) represented by a set of equivalent stiffness coefficients. The procedure involves applying axial force, lateral force, in-plane shear force and lateral shear forces

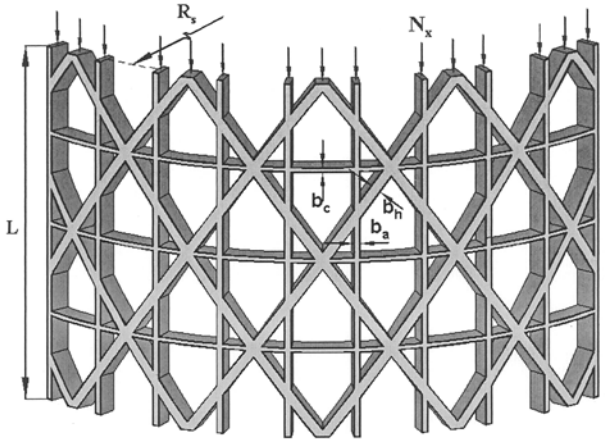

Fig.2 A combination of helical, axial and circumferential stiffening members

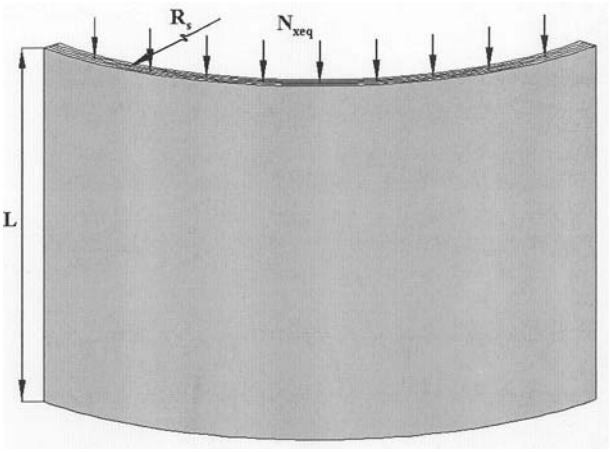

Fig.3 Equivalent plies

independently on the stiffening members as well as on the equivalent shell. These forces are also applied eccentrically w. r. t. the mid plane of the stiffening members. Figs.2 and 3 show the stiffening members and the equivalent plies under axial compression P_x that result the following:

$$N_x = \frac{P_x}{2\, n_h\, b_h / \cos\theta + n_a\, b_a}$$

$$N_{xeq} = \frac{P_x}{2\,\pi\, R} \qquad (19)$$

Expressions for the moment resultants and the remaining stress resultants are obtained by constructing figures similar to Figs.2 and 3. Finally, all stress/moment resultants of the stiffening members are related to those of the equivalent plies and the resulting relations are summarized in Eqn. (20).

$$\frac{N_x}{N_{xeq}} = \frac{M_x}{M_{xeq}} = \frac{N_{xz}}{N_{xzeq}} = \frac{2\,\pi\, R_s \cos\theta}{2\, n_h\, b_h + n_a\, b_a \cos\theta}$$

$$\frac{N_y}{N_{yeq}} = \frac{M_y}{M_{yeq}} = \frac{N_{yz}}{N_{yzeq}} = \frac{L \sin\theta}{2\, n_h\, b_h + n_c\, b_c \sin\theta}$$

$$\frac{N_{xy}}{N_{xyeq}} = \frac{M_y}{M_{xyeq}} = \frac{2\,\pi\, R_s \cos\theta}{2\, n_h\, b_h + n_a\, b_a \cos\theta} \qquad (20)$$

It may be noted that in the above formulation, it is inherently assumed that axial members do not share lateral force and the circumferential members do not share axial force.

Different possible load combinations are applied in Eqn. (13) and Eqn. (15) and comparing the strain energies, elements of the equivalent compliance matrix are obtained. For example, a non-zero load combination of N_x, N_{xeq} would give $A^*_{11eq} = X_1 X_4 A^*_{11}$ other non-zero load combinations are considered and the final expressions for compliance matrices of the equivalent plies are obtained as given in Eqn. (21).

$$\left[\mathbf{A^*_{eq}}\right] = X_4 \begin{bmatrix} X_1 A^*_{11} & X_3 A^*_{12} & X_1 A^*_{16} \\ & X_2 A^*_{22} & X_3 A^*_{26} \\ & Symm & X_1 A^*_{66} \end{bmatrix}$$

$$\left[\mathbf{B^*_{eq}}\right] = X_4 \begin{bmatrix} X_1 B^*_{11} & X_3 B^*_{12} & X_1 B^*_{16} \\ X_3 B^*_{21} & X_2 B^*_{22} & X_3 B^*_{26} \\ X_1 B^*_{61} & X_3 B^*_{62} & X_1 B^*_{66} \end{bmatrix}$$

$$\left[\mathbf{D^*_{eq}}\right] = X_4 \begin{bmatrix} X_1 D^*_{11} & X_3 D^*_{12} & X_1 D^*_{16} \\ & X_2 A^*_{22} & X_3 D^*_{26} \\ & Symm & X_1 D^*_{66} \end{bmatrix}$$

$$\left[\mathbf{S^*_{eq}}\right] = X_4 \begin{bmatrix} X_2 A^*_{44} & X_3 A^*_{45} \\ Symm & X_1 A^*_{55} \end{bmatrix} \qquad (21)$$

The parameters X_1, X_2, X_3 and X_4 are given by :

$$X_1 = \left(\frac{2\pi R_s \cos\theta}{2 n_h b_h + n_a b_a \cos\theta} \right)^2$$

$$X_2 = \left(\frac{L \sin\theta}{2 n_h b_h + n_c b_c \sin\theta} \right)^2$$

$$X_3 = \left(\frac{\pi R_s \sin 2\theta}{(2 n_h b_h + n_a b_a \cos\theta)\ (2 n_h b_h + n_c b_c \sin\theta)} \right)$$

$$X_4 = \left(\frac{\dfrac{2 n_h b_h L}{\cos\theta} + n_a b_h L + 2 n_c \pi b_c R_s}{2\pi RL} \right) \qquad (22)$$

Then, the equivalent stiffness coefficients are obtained by :

$$\begin{bmatrix} \mathbf{A_{eq}} & \mathbf{B_{eq}} \\ \mathbf{B_{eq}} & \mathbf{D_{eq}} \end{bmatrix} = \begin{bmatrix} \mathbf{A^*_{eq}} & \mathbf{B^*_{eq}} \\ \mathbf{B^{*T}_{eq}} & \mathbf{D^*_{eq}} \end{bmatrix}$$

and

$$\begin{bmatrix} \mathbf{A_{eq}} & \mathbf{B_{eq}} & \mathbf{0} \\ \mathbf{B_{eq}} & \mathbf{D_{eq}} & \mathbf{0} \\ \mathbf{0} & \mathbf{0} & \mathbf{S_{eq}} \end{bmatrix} = \begin{bmatrix} \mathbf{A^*_{eq}} & \mathbf{B^*_{eq}} & \mathbf{0} \\ \mathbf{B^{*T}_{eq}} & \mathbf{D^*_{eq}} & \mathbf{0} \\ \mathbf{0} & \mathbf{0} & \mathbf{S^*_{eq}} \end{bmatrix}^{-1} \qquad (23)$$

where

$$\left[\mathbf{A_{eq}}\right] = \begin{bmatrix} A_{11eq} & A_{12eq} & A_{16eq} \\ & A_{22eq} & A_{26eq} \\ & Symm & A_{66eq} \end{bmatrix}$$

$$\left[\mathbf{B_{eq}}\right] = \begin{bmatrix} B_{11eq} & B_{12eq} & B_{16eq} \\ & B_{22eq} & B_{26eq} \\ & Symm & B_{66eq} \end{bmatrix}$$

$$\left[\mathbf{D_{eq}}\right] = \begin{bmatrix} D_{11eq} & D_{12eq} & D_{16eq} \\ & D_{22eq} & D_{26eq} \\ & Symm & D_{66eq} \end{bmatrix}$$

$$\left[\mathbf{S^*_{eq}}\right] = \begin{bmatrix} A_{44eq} & A_{45eq} \\ Symm & A_{55eq} \end{bmatrix} \qquad (24)$$

The equivalent plies together with the plies of the inner/outer skins (if present) constitute an equivalent composite cylindrical shell and global equivalent stiffness

coefficients are obtained by adding the stiffitess matrices of the equivalent plies to those of the inner/outer skins.

Buckling Analysis

Ritz buckling analysis through minimization of total potential energy of the equivalent composite shell is adopted. Transverse shear characteristics are not considered in the classical laminated plate/shell theory but the same are important in a grid-stiffened shell. Formulations following CLST as well as FSDT are used in this study. Given below is a description of the methodologies used in the buckling analysis.

The total potential energy of the grid stiffened composite shell is obtained from Eqn. (10), Eqn. (16) and Eqn. (17). Strain-displacement relations given by Eqn. (2) and Eqn. (5) are used in the energy expressions and the total energy of the shell is expressed as an integrand of generalized displacements. In the case of CLST, these displacements are u_o, v_o, and w_o whereas for FSDT these displacements are u_o, v_o, w_o, ϕ_x, and ϕ_y. These displacements are expressed as kinematically admissible expressions for simply supported boundary conditions as follows [2]:

$$u = \sum_{m=1}^{\infty} \sum_{n=1}^{\infty} U_{mn} \cos \alpha x \quad \cos \beta y$$

$$v = \sum_{m=1}^{\infty} \sum_{n=1}^{\infty} V_{mn} \sin \alpha x \quad \sin \beta y$$

$$w = \sum_{m=1}^{\infty} \sum_{n=1}^{\infty} W_{mn} \sin \alpha x \quad \sin \beta y$$

$$\phi_x = \sum_{m=1}^{\infty} \sum_{n=1}^{\infty} R_{mn} \cos \alpha x \quad \cos \beta y$$

$$\phi_y = \sum_{m=1}^{\infty} \sum_{n=1}^{\infty} T_{mn} \sin \alpha x \quad \sin \beta y \qquad (25)$$

where, $\alpha = \frac{m\pi}{L}$ and $\beta = \frac{n}{R}$

First derivatives of Π w.r.t. U_{mn}, V_{mn} and W_{mn} (in case of CLST) are equated to zero. In the case of FSDT derivatives are also found w. r. t. R_{mn} and T_{mn}. For equilibrium, the total potential energy has to be minimum for which the above derivatives are equated to zero and an Eigen value problem is formed. For different values of α and β different applied loads satisfy the equilibrium equations out of which the minimum load is the critical buckling load.

Parametric Studies

Behavior of a grid-stiffened shell is influenced by a number of variables that necessitates use of quick tools in the preliminary design phase. Smeared stiffener models are efficient in estimating the global buckling failure and in this section influence of various variables on specific buckling load (buckling load per unit length of circumference per unit mass of the shell) of a 500mm diameter shell is studied. Graphical representation of dependence of specific buckling load on the independent variable is made. Discontinuities in the graphs are noticed; these are attributed to changes in the values of the half wave numbers *m* and *n*. As is evident the values of *m* and *n* vary from place to place and for the test cases, covering all the independent variables, carried out in this work these values vary between 1 and 18 for *m* and 1 and 9 for *n*. Material system for the skin as well as the ribs considered in this study is carbon/epoxy with the following values:

E_1 = 170GPa, E_2 = 6.5GPa, G_{12} = 5.6GPa, G_{23} = 2.8GPa, G_{13} = 5.6GPa and ν_{12} = 0.35

Orientation of Helical Ribs

Three different configurations are considered: i) only helical ribs, ii) helical and axial ribs and iii) helical and circumferential ribs. (Fig. 4.) No skin was considered in these configurations.

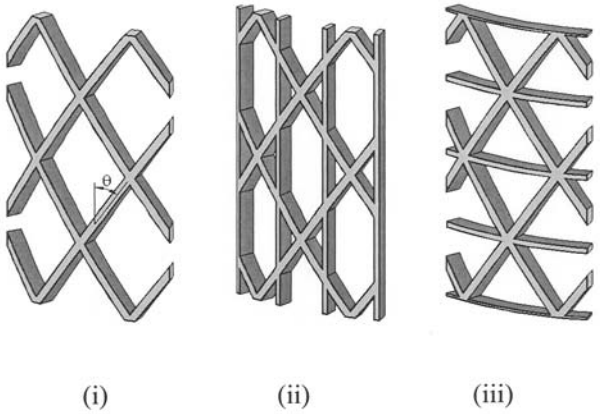

Fig.4 Stiffening rib patterns : (i) Helical ribs only, (ii) Helical and axial ribs, (iii) Helical and circumferential ribs

Angle of orientation (defined as the angle between the local tangent at a point on the helical rib and the local meridian, Fig. 4) of the helical ribs was varied from 5° to 85° and the results are shown in Figs. 5a and 5b. (The choice of the range 5° to 85° is based on the fact that although theoretically helical winding is possible at any angle within the range $0° < \theta < 90°$, θ being the angle of winding, from a practical point of view, helical ribs either at very low angle or at very high angle are i) difficult/impossible to manufacture and ii) not common in most product). It is observed that helical ribs at 30° to 60° result in the highest specific buckling load. Presence of axial ribs and circumferential ribs, in addition to the helical ribs, make the occurrence of specific buckling load skewed towards the high orientation angle and low orientation angle respectively. Also, CLST, as compared to FSDT, consistently overestimates the specific buckling load. This is particularly true when the angle of helical rib is high.

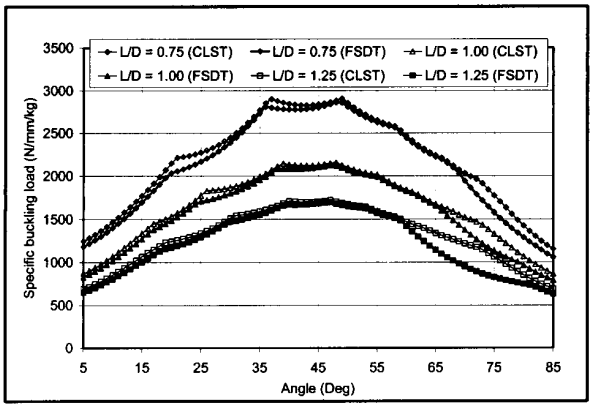

Fig.5a Effect of orientation of helical ribs (only helical ribs without skin)

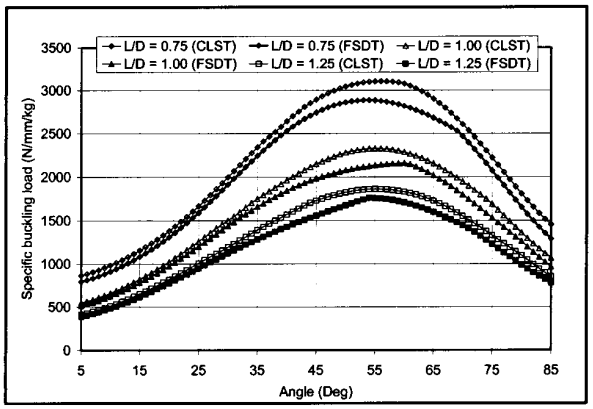

Fig.5b Effect of orientation of helical ribs (helical and axial ribs without skin)

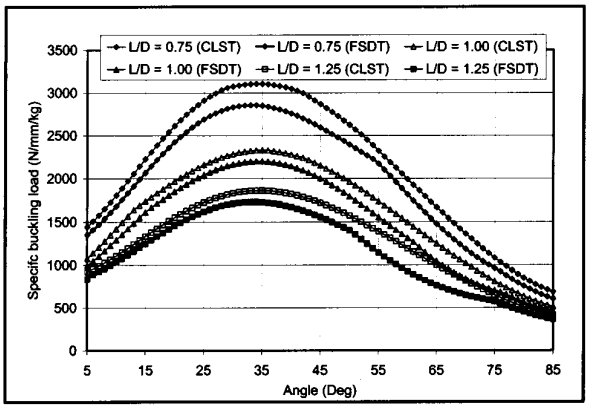

Fig.5c Effect of orientation of helical ribs (helical and circumferential ribs without skin)

L/D Ratio

LID ratios of 0.75, 1.0 and 1.25 are considered. As expected higher L/D ratios, as seen from Figs. 5a, 5b and 5c, result in lower specific buckling load.

Skin Thickness

Three cases of stiffening pattern (as shown in Fig. 4) are considered. However, in addition to the stiffening ribs two skins are also put. The lay-up sequence is: $[90°/+45°/-45°/0°]_s$. (Ply orientation is defined w.r.t. the local meridian). Skin thickness is varied from 0 to 10 mm and the results are shown in Figs.6a to 6c. It is observed that irrespective of the stiffening rib pattern, a lattice structure with stiffening ribs only (i.e. without any skin) is the most efficient shell from specific buckling load. There is a general tendency of specific buckling load to come down to a minimum with gradually increasing skin thickness up

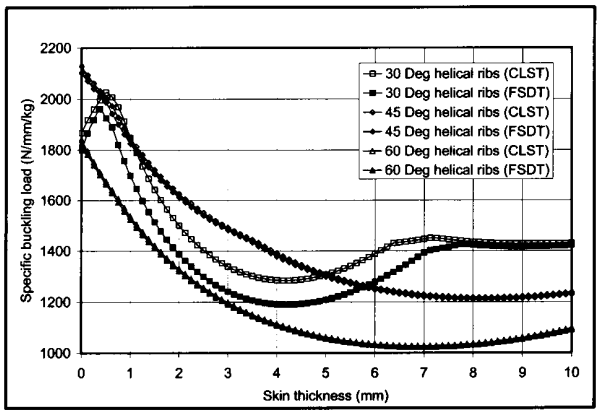

Fig.6a Effect of skin thickness (only helical ribs with two skins)

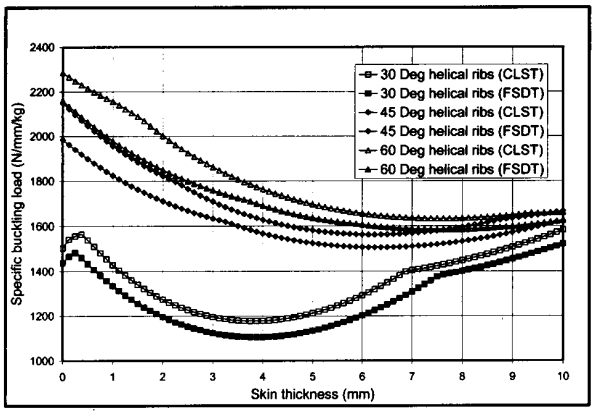

Fig.6b Effect of skin thickness (Helical and axial ribs with two skins)

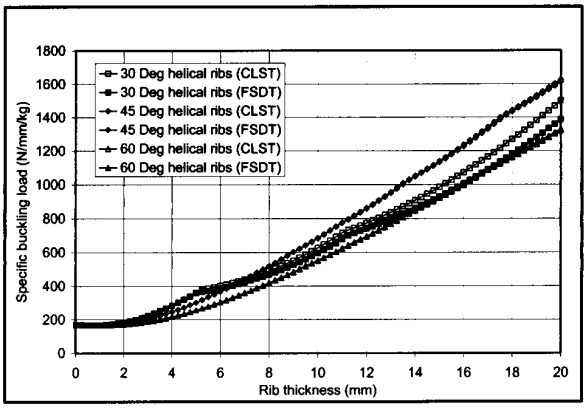

Fig.7a Effect of rib thickness (only helical ribs with two skins)

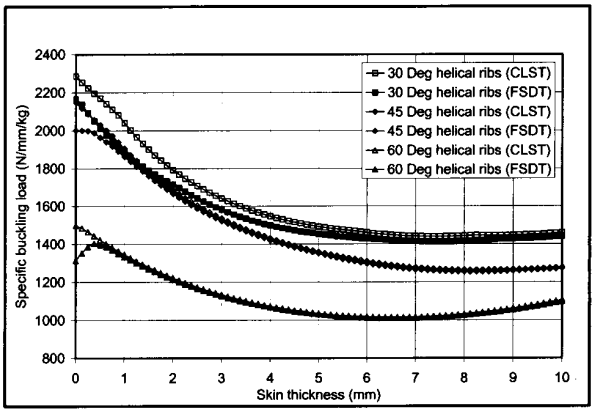

Fig.6c Effect of skin thickness (Helical and circumferential ribs with two skins)

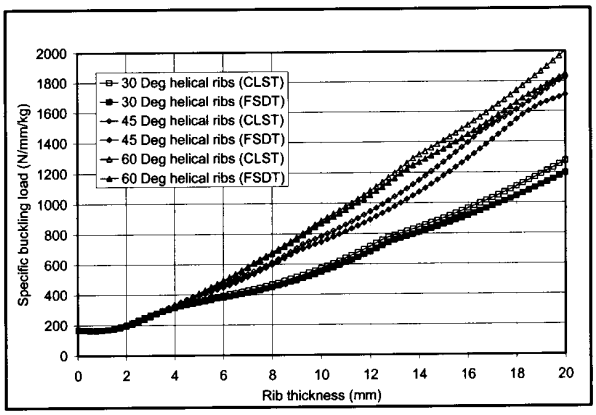

Fig.7b Effect of rib thickness (Helical and axial ribs with two skins)

to about 4mm to 8mm after which specific buckling load increases very gradually with increasing skin thickness. It indicates that addition of a thin skin on to the system of stiffening ribs adds to the overall weight with little addition to the global stiffness characteristics of the shell and thereby the specific buckling load of the shell is reduced. On continuous increase in the skin thickness, total mass of the shell increases but the shell stiffness characteristics improve at a lower rate. As a result, specific buckling load of lattice structure without skin remains the maximum.

Rib Thickness

Configurations same as in the above section are considered here with the difference that here rib thickness is varied from 0 to 10 mm and the skin thickness is kept constant at 2mm. Results are shown in Figs. 7a to 7c. It is observed that the specific buckling loads increase as the

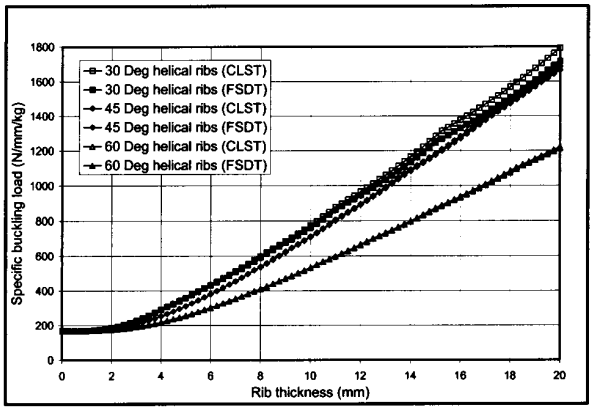

Fig.7c Effect of rib thickness (Helical and circumferential ribs with two skins)

rib thickness increases. It is in the expected line as the stiffness characteristics are greatly improved with increase in rib thickness.

Rib Spacing

Rib spacing depends on the number of helical winding starts. Number of helical winding starts is varied from 3 to 45 for three stiffening rib patterns. For each start, rib spacing is found out based on the angle of helical rib and variations of specific buckling load w. r. t. a/b ratio (ratio of spacing of helical rib to width of helical ribs) are plotted in Figs. 8a to 8c. As is evident from the figures specific buckling load is the highest for the least a/b ratio.

Conclusion

An energy based smeared stiffener model is developed for global buckling analysis of a general grid-stiffened composite cylindrical shell. This analytical method, in the initial design phase, facilitates trying out several combinations of design parameters in an efficient way and thereby the designer can conte to an optimal configuration.

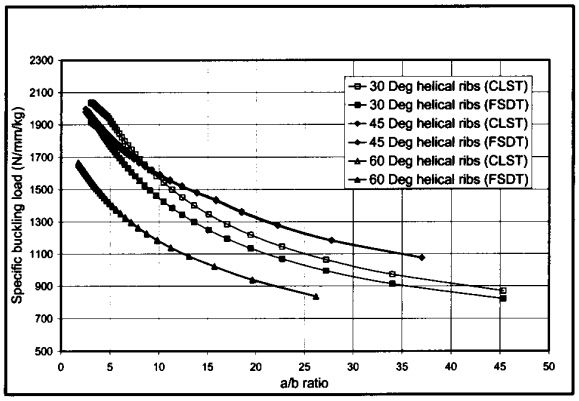

Fig.8a Effect of rib spacing (only helical ribs with two skins)

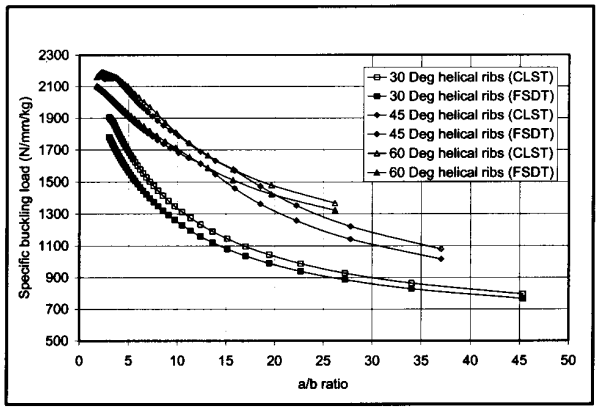

Fig.8b Effect of rib spacing (Helical and axial ribs with two skins)

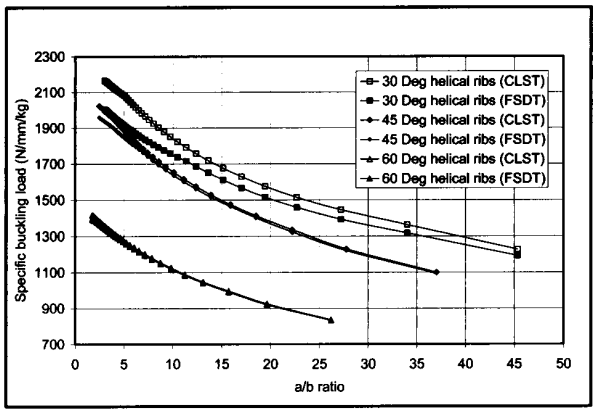

Fig.8c Effect of rib spacing (Helical and circumferential ribs with two skins)

Parametric study is carried out to find out the effects of various design parameters on specific buckling load of the shell. From the point of global buckling, a lattice cylinder without any skin is found to be the most efficient; in other words, minimum skin thickness corresponds to the maximum specific buckling load. On the other hand, specific buckling load is generally proportional to increasing rib thickness. Another fact that comes out is that lower is the rib spacing higher is the specific buckling load.

Ritz energy based approach is adopted in the buckling analysis. Transverse shear properties are important in a stiffened shell and so, First order Shear Deformation Theory, in addition to Classical Laminated Shell Theory, is considered to find out the stiffness matrices. Composites are generally weak in transverse properties that are ignored in CLST but considered in FSDT. It is found that CLST as compared to FSDT, consistently overestimates the specific buckling load of a grid-stiffened cylinder.

References

1. Vasiliev, V.V., Barynin, V.A. and Rasin, A.F., "Anisogrid Lattice Structures - Survey of Development and Application", Composite Structures, 54, 2001, pp. 361-370.

2. Jones, R.M., "Buckling of Circular Cylindrical Shells with Multiple Orthotropic Layers and Eccen-

tric Stiffeners", AIAA Journal, Vol. 6, No.12, 1968, pp. 2301-2305.

3. Wodesenbet, E., Kidane, S. and Pang, S., "Optimization for Buckling Loads of Grid Stiffened Composite Panels", Composite Structures, 60, 2003, pp.159-169.

4. Kidane, S., Li, G., Helms, J., Pang, S. and Woldesenbet, E., "Buckling Load Analysis of Grid Stiffened Composite Cylinders", Composites Part B: Engineering, 34 2003, pp.1-9.

5. Jaunky, N., Knight, N.F. and Damodar, R.A., "Formulation of an Improved Smeared Stiffener Theory for Buckling Analysis of Grid-stiffened Composite Panels", Composites Part B: Engineering, 27B, 1996, pp. 519-526.

6. Jaunky, N. and Knight, N.F., "Optimal Design of Grid-Stiffened Composite Panels Using Global and Local Buckling Analyses", Journal of Aircraft, 35, 1998, pp. 478-486.

7. Damodar, R.A. and Jaunky, N., "Optimal Design of Grid-Stiffened Panels and Shells with Variable Curvature", Composite Structures, 52, 2001, pp.173-180.

8. Slinchenko, D. and Verijenko, V.E., "Structural Analysis of Composite Lattice Shells of Revolution on the Basis of Smearing Stiffness", Composite Structures, 54, 2001, pp. 341-348.

9. Huybrechts, S. and Tsai, S.W., "Analysis and Behavior of Grid Structures", Composites Science and Technology, 56, 1996, pp.1001-1015.

10. Wang, J.T.S., "Discrete Analysis of Stiffened Composite Cylindrical Shells", AIAA Journal, Vol. 23, No. 11, 1985, pp.1753-1760.

11. Jaunky, N. and Knight, N.F., "An Assessment of Shell Theories for Buckling of Circular Cylindrical Laminated Composite Panels Loaded in Axial Compression", International Journal of Solids and Structures, 36, 1998, pp. 3799-3820.

12. Geier, B. and Singh, G., "Some Simple Solutions for Buckling Loads of Thin and Moderately Thick Cylindrical Shells and Panels Made of Laminated Composite Material", Aerospace Science and Technology, 1, 1997, pp. 47-63.

13. Reddy, J.N., "Mechanics of Laminated Composite Plates and Shells", CRC Press.

14. Timoshenko, S.P. and Gere, J.M., "Theory of Elastic Stability", McGraw-Hill Book Company.